

A microscopic image showing a grid of chromosomes. Each chromosome is a circular structure with a central purple spot and a surrounding yellowish ring. Small white arrows point to specific features on the chromosomes. The background is a light brown color.

Manipulating genetic material

by Stefan Thalhammer* and Wolfgang M. Heckl

Over the last 15 years, the use of atomic force microscopy (AFM) has spread from the materials science of hard matter to the fields of biology and biomolecular research. Nowadays, AFM can be used not only as a high-resolution imaging tool for precise cytogenetic studies, but also for the mechanical measurement and manipulation of genetic material. This combination allows, for the first time, identification of sample area, microdissection, and nanoextraction of genetic material for further biomedical and biochemical studies. Here, we show combined AFM and laser-based microscopy techniques, like cutting, gripping, and extracting at the submicron scale, under high-resolution image control and their potential applications in cytogenetics.

Shortly after the 1986 Nobel Prize in Physics was awarded for the invention of the scanning tunneling microscope (STM), Nobel laureate Gerd Binnig, Calvin Quate, and Christoph Gerber built the atomic force microscope (AFM) in order to avoid the limitations of the STM in only imaging conductive matter or thin layers of organics¹ (Fig. 1a). Using the principle of a miniaturized record player, similar to a stylus profilometer, it is possible to image the surface of biological (nonconducting) objects, such as DNA and chromosomes, down to the molecular scale²⁻⁴. The most important fact in the development of the AFM as a universal instrument for bionanotechnology applications is that the tip of the cantilever used for imaging can also be used for measuring forces at the nanoscale, and, moreover, as a nanoscale tool, down to the single-atom level⁵. Here, we show how techniques like cutting, gripping, and extracting biomaterial at the submicron scale under high-resolution image control has been developed into a useful tool, especially in cytogenetic studies (Fig. 1b). The combination of the nanomechanics tool box and modern biochemical techniques like the polymerase chain reaction (PCR) has immense potential in the future development of single-molecule techniques ranging from applications in DNA mechanics to cytogenetic studies and the development of biochips.

Department for Geo- and Environmental Sciences,
GeobioCenter and Center for Nanoscience,
Ludwig-Maximilians-Universität,
Theresienstrasse 41, 80333 München, Germany
*E-mail: s.thalhammer@lrz.uni-muenchen.de
URL: www.nanobiomed.de

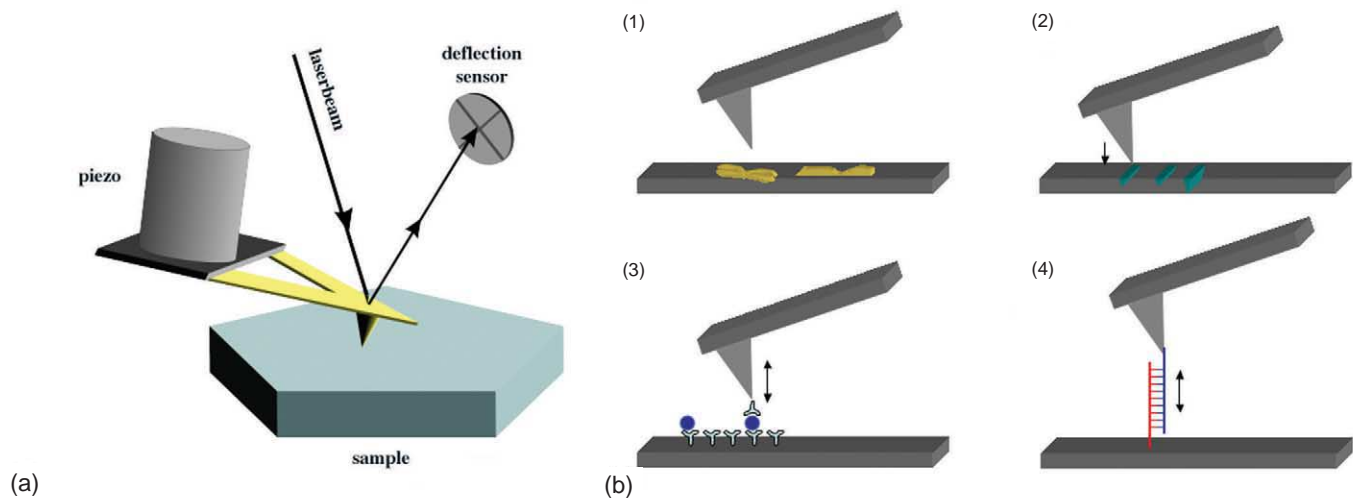


Fig. 1 (a) Setup of an AFM, consisting of a piezo-driven scanner and a laser beam deflection sensor. (b) Different methods for applying AFM in cytogenetics: (1) an imaging tool; (2) a manipulation tool; and (3), (4) as a force sensor. (Reprinted with permission from⁹⁴. © 2004 International Institute of Anticancer Research.)

AFM as an imaging tool

Structural analysis with high resolution not only provides detailed information on high-molecular-weight complexes but can also be used for *in vivo* experiments on biological systems. Data can be recorded in real time. Besides structural information on biological systems, three-dimensional topological data, micromechanical behavior, dynamic processes, and molecular interactions can also be recorded. Table 1 shows a comparison of AFM with other microscopic techniques, together with the required sample preparation.

Cytogenetics is basically a visual science. Established microscopic techniques, such as light and electron microscopy, have been used widely for the study of

chromosomes. Since its invention, AFM has been applied in different fields of genetics. Double-stranded DNA fixed on freshly cleaved mica has been imaged in air by several groups^{7,8}. Hansma and coworkers⁹ have successfully imaged plasmid DNA fixed on mica in propanol. By adding new spreading chemicals, e.g. quaternary ammonium salts, it has been possible to reduce surface impurities, and the surface density of the molecules can be measured reproducibly¹⁰. After the introduction of the tapping mode, it became possible to image DNA with fewer potentially destructive shear forces during scanning, which has resulted in a more detailed image of the macromolecule¹¹. In Fig. 2a, we have imaged a double-stranded plasmid, pUC19, using the tapping

Table 1 Comparison of different microscopic techniques to image sample topography, e.g. metaphase chromosomes⁶.

	Conventional optical microscopy	Scanning electron microscopy (SEM)	Field-emission in-lens scanning electron microscopy (FEISEM)	Atomic force microscopy (AFM)
Microscopic environment	ambient, liquid, vacuum	vacuum	vacuum	ambient, liquid, vacuum
Field depth	small	high	medium	medium
Focus depth	medium	small	very small	small
Resolution:				
<i>x, y</i>	100 nm	5 nm	0.7 nm	0.1-1.0 nm
<i>z</i>	n/a	n/a	n/a	0.01 nm
Magnification	1x – 2x10 ³ x	10x – 10 ⁶ x	9x – 10 ⁵ x	5x10 ² x – 10 ⁸ x
Necessary sample preparation	low	critical-point drying or freeze-drying, coating	critical-point drying if necessary	low
Necessary sample properties	samples do not have to be completely transparent for visible light	samples should not charge and have to be vacuum compatible	vacuum compatibility	samples should not have excessive changes in height compared to tip geometry

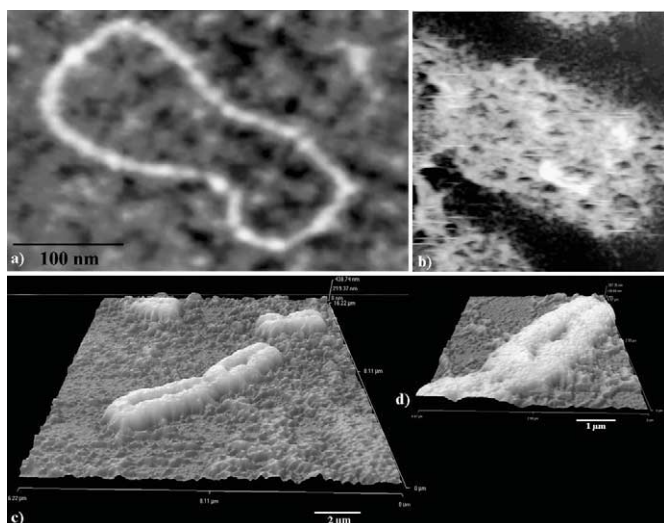


Fig. 2 (a) AFM image of plasmid pUC19 (~2.7 kbp) diluted in deionized H₂O, deposited by spin stretching, and imaged in tapping mode in air (bar: 100 nm). (b) Metaphase chromosome after proteinase K digestion; a fibrous network is clearly detectable. (c) Three-dimensional AFM image (recorded in contact mode) of untreated human chromosomes (bar: 2 μm). (d) AFM enhancement of the p-arm of the recorded chromosome (bar: 1 μm). (Reprinted with permission from²⁴. © 2004 International Institute of Anticancer Research.)

mode in air. DNA in a higher condensation status in sperm cells was imaged by Allen and coworkers¹² in air and in liquids. Furthermore, structural experiments on chromatin fibers¹³, as well as volume determinations on metaphase chromosomes in air¹⁴ and liquids¹⁵ have been performed.

Structural examinations on metaphase chromosomes have been performed by Heckl², where the comparison to electron microscopy was also made, and later by de Groot and Putman¹⁶ and Rasch *et al.*¹⁷. Figs. 2c and d show untreated human metaphase chromosomes. A GTG-like banding pattern (see Glossary) has been observed in topographical images of metaphase chromosomes untreated by chemicals or enzymes¹⁸. The GTG banding, obtained by digesting the chromosomes with proteolytic trypsin followed by Giemsa staining, is the most widely used in routine chromosome analysis. Metaphase chromosomes imaged by AFM have revealed structures similar to those reported in light and electron microscopy. Depending on the preparation technique, substructural details can be recorded in metaphase chromosomes^{19,20}. After pepsin digestion of the metaphase chromosomes, a granular substructure is detected in contact mode. In this case, not only the covering plasma layer but also scaffold-stabilizing proteins are digested. The recorded details represent a nucleosomal structure, which has been discussed by several authors^{16,21-23}. The recorded data are comparable to those generated by scanning electron

Glossary

- **CBG bands:** C bands are obtained by using Ba(OH) and Giemsa staining. The C-banding technique produces selective staining of constitutive heterochromatin. These bands are located mostly at the centromeric regions of chromosomes, hence the term C bands.
- **FISH:** Fluorescence *in situ* hybridization. A technique whereby small lengths of DNA (probes), which 'recognize' complementary DNA on particular chromosomes or parts of chromosomes, are labeled with a colored fluorescent dye and then used to highlight 'target' DNA in chromosomes. This technique vividly paints chromosomes or portions of chromosomes.
- **GTG bands:** G bands are obtained by digesting the chromosome with proteolytic enzyme trypsin then Giemsa staining, giving a chromosome-specific banding pattern of light and dark (positive and negative) bands.

microscopy²⁴. Metaphase chromosomes consist of 30 nm fibers folded in a tandem array of radial loops, which are packaged into a fiber with an overall diameter of 200-250 nm. High-resolution AFM images of metaphase chromosomes reveal structural features in the size range of 30-100 nm, which correspond to the loops of the 30 nm fiber¹⁶. Other authors^{21,25} have reported features as small as 10-20 nm, which could correspond to individual nucleosomes. When scanning in contact mode, the tip of the AFM can be contaminated by unwanted pickup of chromosomal material. The material adhering to the tip can limit its use for manipulation and microdissection experiments (see section below). In noncontact mode, the tip scans over the chromosomal surface at a distance of a few hundred angstroms. The tip is not in contact with the sample surface and, therefore, does not get contaminated while scanning. The advantages and disadvantages of these two operating modes are combined in tapping mode²⁶, in which the tip is in periodic contact with the chromosomal surface. In addition, lateral force microscopy has been used to get a deeper look inside chromosomal organization²⁷.

In summary, the operation modes described can be used for imaging chromosomal material and recording substructure, depending on the sample preparation. The topography of the metaphase chromosomes is preserved and not deformed^{16,18}. Table 2 summarizes the properties of contact, noncontact,

Table 2 Properties of the different operation modes in AFM for high-resolution imaging, manipulation, and microdissection of metaphase chromosomes.

Operation mode	Contact mode	Noncontact mode	Tapping mode
Tip loading force	low → high	low	low
Contact with sample surface	yes	no	periodical
Manipulation of sample	yes	no	yes
Contamination of AFM tip	yes	no	yes
Microdissection	yes	no	no

and tapping modes for the high-resolution imaging and manipulation of metaphase chromosomes.

By using specific *in situ* hybridization techniques, distinct areas of hybridization can be detected in metaphase chromosomes. Biotinylated DNA probes can be used for mapping, and the specific sites visualized by detecting changes in topography induced by a peroxidase-diaminobenzidine reaction^{17,28}. Using the same detection technique, Kalle and coworkers²⁹ are able to identify specific signals after RNA *in situ* hybridization. In studies on cereal chromosomes, a genome-specific probe was used. AFM imaging detected changes in height as a result of biotin-avidin-fluorescein isothiocyanate complexes, formed as a consequence of fluorescence *in situ* hybridization (FISH) procedures²⁵. *In situ* hybridization with subsequent detection of the specific DNA probe has been performed in our group³⁰. The specific hybridization signal is detected using 5 nm Au particles with subsequent Ag enhancement (see Fig. 3d).

The AFM can also image genetic material in liquids. The viscoelastic properties of rehydrated chromosomes and volume determinations in liquids have been recorded by AFM^{23,31}. Compared with light or electron microscopy, the AFM is able to operate in liquids and to perform local measurements on any point of the sample surface³². Thus, data on the biophysical properties of metaphase chromosomes can be obtained.

Chromosome-banding techniques have facilitated the precise identification of individual chromosomes. Interpretation of the origin of GTG bands is still in progress. A direct role of Giemsa stain in producing the GTG bands has been suggested³³. Several authors infer that chromosomes contain a preexisting structure that is enhanced by GTG banding. But it is still unclear how this enhancement occurs^{34,35}. It is hypothesized that the differences between positive and negative GTG bands may be induced by the spatial organization of chromosomal protein and DNA.

Unlike light microscopy, no changes in color can be detected in AFM, only differentiation of topographical

information within the metaphase chromosome. The resulting image is not only the result of topographical changes in the chromosome surface, but also of the interaction of the tip with the viscoelastic properties of the chromosome. Fig. 3a shows a topographic AFM image of a GTG-banded chromosome 7 homolog. The morphology of the chromosome is preserved; the banding pattern and the fibrous nature is detectable. Structural protrusions along the chromosome corresponding to the dark bands in Fig. 3a are detectable. A linescan of the q-arm shows differences in height between dark and light bands of about 90 nm. The length of the ridges is about 540 nm. It is known from chromosomes imaged by SEM that the Giemsa light and dark bands differ in height³⁶. One must be aware that the AFM image not only represents the topology of the sample surface

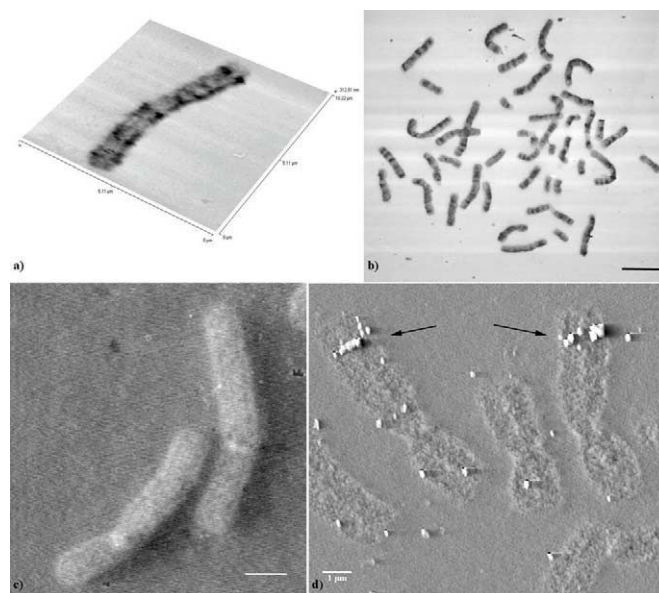


Fig. 3 (a) AFM image of a GTG-banded chromosome 7 homolog. In the topographic AFM image (gray scale inverted), the bright and dark banding pattern is detectable. (b) AFM image of a (karyotype: $2n = 46, XX$) female GTG-banded metaphase spread (bar: 10 μm). (c) AFM image of CBG-banded metaphase chromosomes spread (see Glossary) with highlighted centromeric region (bar: 2 μm). (d) AFM error-signal image of *in situ* hybridized human metaphase chromosomes after detection using 5 nm Au particles with subsequent Ag enhancement. The probe used was MLL 11q23, a probe to detect the majority of rearrangements at the MLL gene locus (see arrows) that are frequently associated with human myeloid and lymphoid leukemia (bar: 1 μm). (Reprinted with permission from⁹⁴. © 2004 International Institute of Anticancer Research.)

but also the compressibility of the sample, therefore height is partially expressed as topography. Fig. 3b shows a human $2n = 46, XX$, female metaphase spread. The light and dark bands are clearly detectable and all chromosomes can be identified.

It is possible to identify features equivalent to G-banding patterns in untreated chromosomes and to use these for classification¹⁸. As in light microscopy, dark and light bands can be correlated in GTG-banded chromosomes and can be classified accordingly³⁷. In former AFM studies, G-positive bands were found to be areas with a higher surface relief¹⁷.

After more than 20 years, the banding mechanism is still unknown. None of the biochemical and physical reactions are understood. The banding patterns allow the specific classification of chromosomes. The comparison of unstained and Giemsa-stained chromosomes by phase-contrast microscopy^{33,38} set up the hypothesis that staining techniques amplify a preexisting incomplete structural organization of chromatin. Electron microscopy supports this hypothesis^{39,40}. McMaster and coworkers⁴¹ suggest that the stains influence structure and morphology, based on their work on untreated metaphase chromosomes. In SEM, light and dark bands in the R bands (reverse bands produced by heating using Giemsa) and the G-banding pattern can be differentiated by changes in height³⁶. This suggests that, at least in this instance, high-resolution AFM allows an intrinsic banding pattern to be visualized that otherwise has to be enhanced by accumulation of stains for viewing with light-microscopy methods. The accuracy of chromosomal banding is strongly related to DNA organization and the associated proteins. AFM images in air and liquids of RNase-, pepsin-, or trypsin-treated chromosomes suggest that the level of organization consists of a radial arrangement of chromatin loops, which are anchored to a folded fiber, giving a pattern of bands differing in volume. Furthermore, a model derived from these data links genome sequence, cytogenetics, and chromosome structure^{42,43}.

The C-banding technique produces selective staining of constitutive heterochromatin. These bands are mostly located at the centromeric regions of chromosomes, hence their name C bands. The original method described by Arrighi and Hsu⁴⁴ primarily involves treatment with an alkali (sodium hydroxide) to denature the chromosomal DNA and subsequent incubation in a salt solution. Another method, described by Sumner⁴⁵, uses a milder alkali (barium

hydroxide). Both methods produce similar characteristic C-banding patterns. Fig. 3c shows an AFM image recorded in contact mode of CBG-banded metaphase chromosomes. In comparison to light microscopic images, the stained centromeric regions are clearly detectable. CBG-banding for studying chromosome rearrangements near centromeres and for investigating polymorphisms was performed using AFM by Tan and coworkers⁴⁶.

A detailed understanding of nuclear cell functions requires an accurate knowledge of the spatial organization of nuclear structures. SEM provides higher resolution than light microscopy and permits surface analysis of the chromosomal structure, which cannot be adequately obtained from transmission electron microscopy (TEM). Nevertheless, to obtain high resolution in SEM observations, the use of a high electron accelerating voltage (up to 30 kV) is required⁴⁷⁻⁴⁹. Under these experimental conditions, sputter-coating or conductive staining of the samples is generally required⁵⁰. Both procedures allow electron-charging dispersion from the sample but may obscure fine details and alter the sample⁵¹. Today, only a few techniques are available for high-resolution imaging of chromosomal material with few artifacts, such as the field-emission in lens scanning electron microscope (FEISEM) and the AFM. The FEISEM is a special kind of SEM fitted with a cold-cathode, field-emission electron gun^{52,53} that can operate at a low accelerating voltage with reduced electron charging of the sample. In fact, the low-voltage and low-current electron beam of the FEISEM, together with a liquid nitrogen anticontamination device close to the specimen area and 'in lens' assembly of the electron-optic column, allows high-resolution imaging of the biological sample without any conductive staining or metal coating. Contamination of the specimen is highly reduced compared with conventional SEM⁵². The sample location between the objective pole pieces limits the dispersion of the secondary electrons collected by the magnetic field of the lens. In conclusion, these characteristics allow the observation of uncoated biological samples with a higher resolution than with conventional SEM⁵⁴⁻⁵⁷.

FEISEM and AFM microscopy can be combined to observe the same metaphase chromosome samples obtained from standard cytogenetic preparations of human HL60 cells. After cleaning, the metaphase spreads via different procedures⁵⁴. The analysis of the same samples was facilitated by the use of conductive glass (ITO glass) for the chromosome map

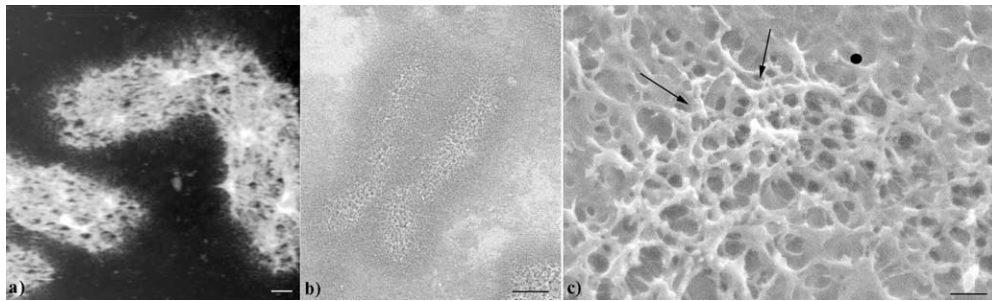


Fig. 4 Human metaphase chromosomes after proteinase K treatment. (a) AFM image (bar: 1 μm). (b) FEISEM image of a comparable chromosome. A dark halo surrounds the entire chromosome (bar: 1 μm). (c) Increasing the magnification, the chromosomal surface appears to constitute a network. Some fibrillar structures parallel to the axis of the chromatid are detectable (arrows). The halo around the chromatid appears to be formed by a mix of fibers and a homogeneous phase (dot) (bar: 100 nm). (Reprinted with permission from⁹⁴. © 2004 International Institute of Anticancer Research.)

preparation. These two different technical approaches show a high correlation of the respective morphological information, both in normal and treated samples. The high-resolution potential of the FEISEM, together with the possibility of observing hydrated samples and/or nanomanipulating the specimen with the AFM, confirm morphological data and offer enhanced information on their biological significance (Fig. 4)²⁰.

Nanomanipulation and microdissection of genetic specimens

Precise manipulation and microdissection of genetic material can help to design chips for genetic analysis and develop biosensors and lab-on-a chip diagnostic devices.

Nanomanipulation can be defined as the manipulation of nanometer-size objects with nanometer-size actuators and with nanometer precision⁵⁸. Manipulation means that objects are pushed, pulled, positioned, assembled, cut, etc. by controlling external parameters. Based on the different type of interactions, biological nanomanipulation can be divided into mechanical contact, optical, electrical, and fluidic noncontact, and hybrid systems (see Fig. 5).

In this section, we focus on the possibility of using nanomanipulation systems as microdissection tools in genetics. Mechanical AFM microdissection and noncontact ultraviolet (UV) laser microdissection will be discussed. The applications range from structural analysis to the generation of molecular probes.

Initially, microdissection of genetic material was performed with extended glass needles. This mechanical approach, in which the tip of the needle is in contact with the sample, allows the dissection of material in the range of 1 μm . The tip of an AFM cantilever can be used to scale the dissection

method down to the nanometer range. Here, the tip is used for manipulation and microdissection instead of imaging.

The first experiments, which used extended glass needles, were performed on polytene chromosomes of *Drosophila melanogaster*⁵⁹. The method was transferred to mammalian and human chromosomes⁶⁰⁻⁶³. The aim of these experiments was the integration of the isolated chromosomal fragments into vectors for subsequent cloning. They were limited by the small amount of DNA available. This was overcome by the development of PCR. One possibility was the introduction of primer-specific sequences, which were ligated to the microdissected DNA^{64,65}. These highly region-specific probes are extremely valuable for molecular cytogenetic studies as well as for positional cloning projects. With improvements in mechanical microdissection techniques using extended glass needles and PCR, there are two distinct methods for generating a chromosome library from microdissected chromosomal DNA: direct cloning⁶¹ and PCR-mediated cloning⁶⁶⁻⁶⁸. Depending on the primer, the latter method is

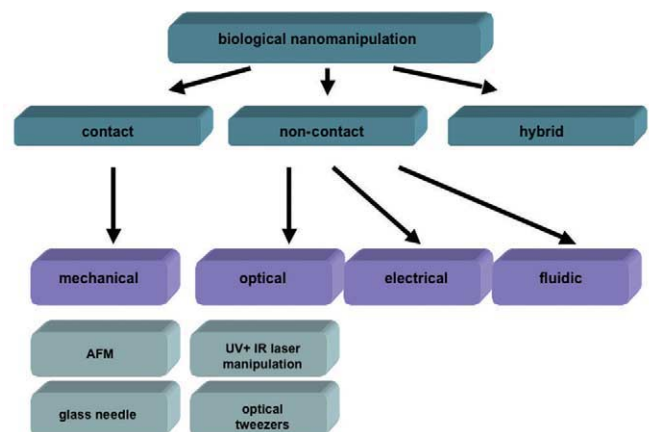


Fig. 5 Overview of biological nanomanipulation types.

divided into degenerate oligonucleotide-primed PCR using random primers^{67,69,70} and vector- or adaptor-mediated PCR with specific primers^{66,71,72}. Many protocols for the PCR amplification of DNA from few or even single cells have been published in the last few years. These include primer-extension preamplification⁷³, degenerate oligonucleotide-primed PCR⁶⁷ and Alu-PCR⁷⁴. They are of variable complexity and none have convincingly demonstrated the homogenous amplification of the genome of a diploid cell, although some are quite useful for various cytogenetics analyses^{75,76}. Linker-adaptor PCR can overcome this problem. Chromosome microdissection and amplification of the isolated fragments by Mbol-linker-adaptor PCR for genetic disease analysis was described in the early 1990s⁷⁷. This method uses specific linkers ligated to the ends of DNA fragments, generated by restriction enzyme digestion; DNA is then amplified using PCR primers homologous to the linker-adaptor oligonucleotide. By combining linker-adaptor PCR and comparative genome hybridization, it is possible to detect loss of heterozygosity in single isolated cells⁷⁸.

A noncontact technique of laser-based microdissection of entire chromosomes and chromosomal fragments has been demonstrated⁷⁹. By combining PCR, cloning techniques, and laser microdissection, it is possible to generate region-specific chromosomal probes for molecular cytogenetics⁸⁰⁻⁸². But the chromosomal fragments have to be collected with an extended glass needle after laser microdissection. The generation of chromosomal-specific painting probes has been reported with an entire noncontact laser-based microdissection in single and multicolor FISH experiments⁸³⁻⁸⁵ (Fig. 6).

Since the invention of the AFM and its use in structural biology of chromosomes, research has focused on its use not only as an imaging tool but also as a manipulation tool. By combining high structural resolution with the ability to control image parameters at any position within the scan area, it is



Fig. 6 (a), (b) Laser-based microdissection and isolation of a single metaphase chromosome fixed on a supporting membrane (see arrow). (c) Human chromosome 3 specific paint probe, generated from a single isolated chromosome (see arrows). (Adapted from⁸⁵.)

possible to use the AFM as a micromanipulation tool. Hoh and coworkers⁸⁶ have demonstrated the possibility of using the AFM as a microdissection device. They performed microdissection on gap junctions between cells. Controlled nanomanipulation of biomolecules has been performed on genetic material⁹. Fragments of 100-150 nm have been cut out of circular plasmid DNA. Isolated DNA adsorbed on mica has been dissected in air^{9,87,88} and in liquids, e.g. propanol⁹, by raising the applied force to ~5 nN at the AFM specimen. These experiments demonstrate the feasibility of microdissection in the nanometer range. By combining AFM imaging and microdissection, the organization of bovine sperm nuclei can be observed, showing small protein and DNA-containing subunits with diameters of 50-100 nm¹². A tobacco mosaic virus has been dissected and displaced on a graphite surface to record the mechanical properties of virus binding⁸⁹.

Chromosomal dissection allows direct isolation of selected regions. Therefore, it can be used to build chromosome-band libraries⁶⁴ for cytogenetic mapping strategies or specific cloning projects. AFM microdissection of genetic material in a different condensation status, such as polytene chromosomes of *Drosophila melanogaster*, has been performed by Henderson's group^{90,91}. The cut size achieved in chromosomal regions is 107 nm. Depending on the shape of the AFM tip, the size increases to 170 nm in larger regions. Furthermore, human metaphase chromosomes have been microdissected and the extracted material used for subsequent biochemical reactions^{75,92,93}. Manipulation of mouse chromosomes has been described. After dissection with a modified AFM tip, the collected material is amplified with subsequent Southern hybridization of the extracted single-copy DNA⁹². AFM microdissection in dynamic mode for the chemical and biological analysis of tiny chromosomal fragments has been shown. In this approach, the marker gene of the nucleolar organizing region (NOR) was amplified by designed primers for 5.8S ribosomal DNA after performing a series of single-line scan microdissections. The dissected chromosomal fragments are collected in a second step with a conventional microcapillary⁹³. Human metaphase chromosomes have been dissected at selected regions by upstream noncontact imaging of GTG-banded metaphase chromosomes. The microdissection process can be recorded^{37,75}. In this direct approach, the extracted genetic material adhering to the tip was amplified by an unspecific polymerase chain reaction. Then the material can be used as

a probe for FISH⁷⁵. As described, AFM can also be operated in liquid environments. But microdissection in liquids produces only uncontrolled cuts on rehydrated chromosomes³².

The combination of high-resolution imaging and manipulation allows, for the first time, identification of the sample area, microdissection, and nanoextraction of genetic material at once. This nanometer-sized material can be used for further biomedical and biochemical studies⁹⁴.

AFM nanoextraction procedure

The procedure for AFM-based micro- and nanodissection is as follows^{75,95,96}. To avoid contamination, all steps are performed under sterile conditions. To identify the chromosomal region of interest for isolation, and to minimize contamination of the AFM tip while scanning the area of interest, GTG-banded metaphase chromosomes are imaged in noncontact mode in ambient air (see Figs. 7a and b). Identification can also be performed with a 'preset' *in situ* hybridization of chromosome-specific painting probes. The chromosome can be identified via fluorescence microscopy⁷⁵ or AFM-particle detection (Fig. 3d). This 'preset' hybridization also increases the amount of extracted genetic material.

For microdissection, the chromosome is placed at a 90° angle to the scan direction and the chromosomal area is zoomed in on. For distance control, amplitude detection is

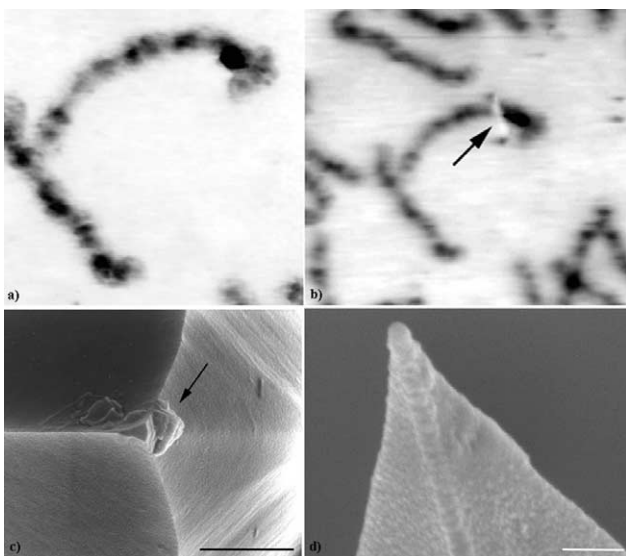


Fig. 7 (a) Noncontact AFM image of the GTG-banded human chromosome 7 before microdissection. (b) AFM microdissection of the band 7q32 (see arrow). (c) Electron microscopy image of the AFM tip after microdissection. The arrow indicates the extracted DNA (bar: 1 μm). (d) Electron microscopy image of an electron-beam-deposited rough AFM tip to increase the extraction efficiency (bar: 200 nm). (Reprinted with permission from⁹³. © 2004 International Institute of Anticancer Research.)

used and the damping level is set to 50% of the amplitude of free oscillation for imaging before extraction. After identification of the extraction site, scanning is stopped and the feedback turned off. The loading force of the tip onto the sample is increased. Figs. 8a-e show the results of AFM microdissection by applying different loading forces to the specimen and by controlling the modulation of the z-piezo drive. Depending on the applied loading force, the micromanipulation of the metaphase chromosome results in a microindentation or microdissection (see Figs. 8b-c).

To extract DNA, a single linescan at a speed of 1 $\mu\text{m}/\text{sec}$ is performed at the desired site. During dissection of the chromosome, the lateral forces play an important role. The tip performs a stick-slip movement and the forces between the tip and chromosome are reduced while operating with z-modulation. The shear forces of the tip are reduced during dissection and reproducible cuts of 100 nm are possible, depending on the geometry of the tip. By changing the tip after each microdissection, serial cuts can be performed (see

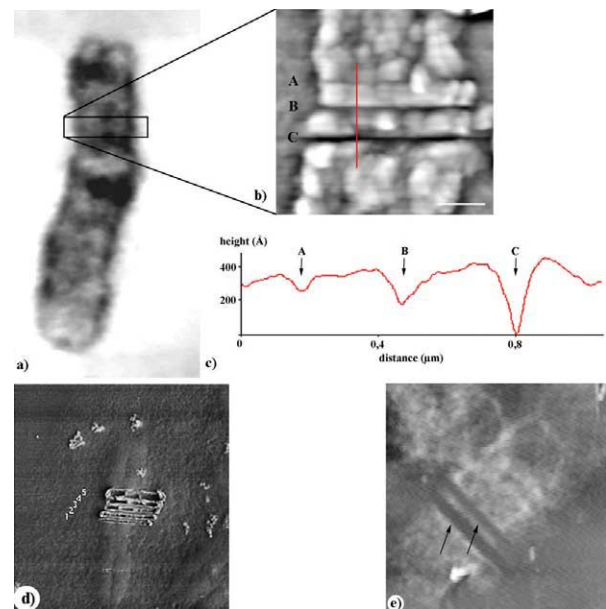


Fig. 8 (a) GTG-banded human chromosome 9 imaged in noncontact mode, frame marks the area of a series of microdissections. (b) The chromosomal area was imaged by AFM in ambient conditions after a series of dissections made by AFM. For dissection, z-modulation (~ 5 nm) has been used. The oscillation amplitude of the cantilever was smaller than 1% of the amplitude of free oscillation for all cuts. Each cut was performed using one linescan at 1 $\mu\text{m}/\text{s}$ with a setup loading force of: A, 7 μN ; B, 9 μN ; and C, 13 μN (bar: 500 nm). (c) Cross-sectional analysis along the red line indicated in (b). The applied force results in an indentation (A, 7 μN ; B, 9 μN) and total dissection of the metaphase chromosome (C, 13 μN). (d) Electron microscopy image of human metaphase chromosome after microdissection with vertical modulation of the z-piezo drive. Loading forces are: 1, 16.8 μN ; 2, 19.6 μN ; 3, 22.4 μN ; 4, 25.6 μN ; and 5, > 27 μN . (e) Serial microdissections with the AFM, arrows mark the dissections. (Reprinted with permission from⁹³. © 2004 International Institute of Anticancer Research.)

Fig. 8e). During microdissection, not only the apex but also the flank of the tip is in contact with the chromosome. Thus, the loading area to the chromosome is increased and, under constant force, the loading force applied to the tip is decreased. The chromosomal material is not dissected in a first step but pushed, as with a snowplough. Parts of the chromosomal material adhere to the tip via van der Waals interactions and unspecific adsorption. Electron-beam-deposited (EBD) tips with a rough surface can be used to increase the extraction efficiency³⁰ (see Fig. 7d). The modified AFM tips can be used as a mechanical 'nanoscalpel' or a 'nanoshovel'. As shown above, the influence of the physical parameters used for nanomechanical dissection is important for the result. Nanostamping by applying an oscillatory vertical movement of the tip, while cutting in horizontal direction, is most important to avoid pure horizontal tearing of the chromosome instead of precise cutting and extracting³².

After the tip is retracted from the sample surface, the cantilever is transferred into a reaction tube. A new cantilever is used to check the cut at the nanoextraction site on the chromosome. The reaction tube contains a collection buffer to stabilize the extracted genetic material. Enzymatic digestion of the chromosome-stabilizing and -covering proteins is performed to increase primer binding and, therefore, the efficiency of PCR. Unspecific amplification can be performed with PCR techniques using degenerate primers⁷⁵ or linker-adaptor PCR³⁰. The genetic samples generated can be used for further cytogenetic studies, e.g. FISH⁷⁴ or amplification of specific target sequences³⁰.

Microdissection has been performed by AFM combined with laser cutting. In a specially designed experimental setup, the minimum cut sizes of human metaphase chromosome achieved by a laser (on the order of 500 nm) are compared with AFM-tip cuts (as small as about 100 nm)⁷⁵. This shows the advantage of AFM technology with respect to precision toward single-molecule manipulation⁹⁷. In addition, the integrated setup allowed *in situ* characterization of laser cuts far below the diffraction limit of light in light microscopy.

Conclusion and outlook

More than ten years ago, with the advent of the AFM, we stated that its ease of use and the possibility of investigating real-time dynamics of biological objects in a liquid environment could make it a promising tool for new insights into biological mechanisms and structures in the future⁴.

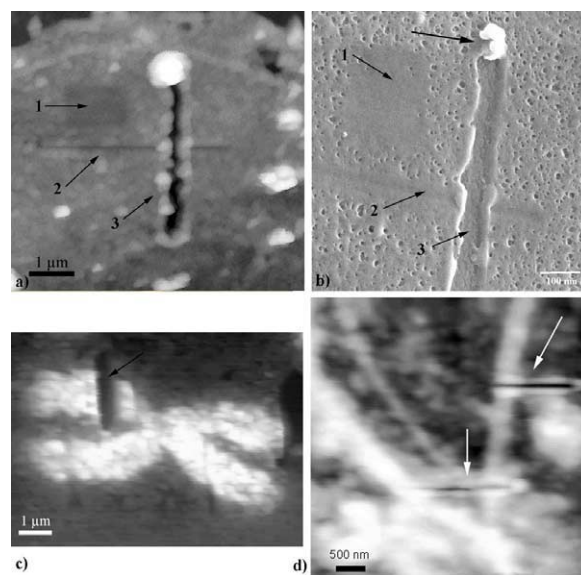


Fig. 9 AFM microdissection of (a) an interphase nucleus and (b) the corresponding electron microscopy image. Increasing forces from 1 to 3 cause indentation or microdissection; the large arrow indicates the remaining compressed genetic material during extraction. (c) Microdissection of a single chromatid (see arrows), and (d) microdissection of extended chromatin fibers (see arrows). (Reprinted with permission from⁹³. © 2004 International Institute of Anticancer Research.)

Based on its working principle, the AFM can not only be used for high-resolution imaging of surface topography of genetic material but also, at the same time, it is a perfect tool on the nanometer scale. In addition to high structural analysis and recording of the tip torsion while manipulating the surface structure (see Fig. 9), it is possible to record the three-dimensional structure of genetic material, e.g. metaphase chromosomes or interphase nuclei. When AFM microdissection is applied on different genetic samples, like extended chromatin fibers (Fig. 9d) or single DNA plasmid molecules, it is possible to isolate the smallest cytogenetic samples³⁰. Subsequently, the DNA can be further processed by highly sensitive PCR and FISH for physical mapping of the genome, evolutionary studies, or diagnostic research. In the future, it will be interesting to use a near-field optical microscope to identify a particular genomic region labeled with just a few dye molecules for subsequent nanodissection, or to use more sophisticated and smaller detection markers for localizing the gene region to be extracted. ■

Acknowledgments

The authors would like to thank U. Köhler (MGZ Munich), J. Geigl and S. Langer (TU Munich), and L. Costa and H. Meimberg (LMU Munich) for cooperation. Valuable contributions by G. Wanner, H. Lorenz (LMU Munich), P. Gobbi (Uribino, Italy), and G. Teti, M. Falconi, and G. Mazzotti (Bologna, Italy) concerning electron microscopy studies are recognized. This work was supported by a Deutsche Forschungsgemeinschaft (DFG) SFB 486 grant.

REFERENCES

1. Binnig, G., et al., *Phys. Rev. Lett.* (1986) **56** (9), 930
2. Heckl, W. M., *Thin Solid Films* (1992) **210-211**, 640
3. Heckl, W. M., and Engel, A., *Imaging Nucleic Acids with Scanning Probe Microscopes*, In *Visualization of Nucleic Acids*, Morel, G., (ed.), CRC Press, Boca Raton, USA (1995), 21
4. Heckl, W. M., In *The Diagnostic Challenge, The Human Genome*, Fischer, E. P., and Klose, S., (eds.), Piper, Munich (1995), 99
5. Heckl, W. M., In *Pioneering Ideas for the Physical and Chemical Sciences*, Fleischhacker, W., and Schönfeld, T., (eds.), Plenum, New York (1995), 179
6. Thalhammer, S., et al., In *Atomic Force Microscopy, Biomedical Methods and Applications*, Braga, P. C., and Ricci, D., (eds.), Humana Press, New York (2003), 245
7. Thundat, T., et al., *Ultramicroscopy* (1992) **42-44** (2), 1101
8. Yang, J., and Shao, Z., *Ultramicroscopy* (1993) **50** (2), 157
9. Hansma, H. G., et al., *Science* (1992) **256**, 1180
10. Schaper, A., et al., *FEBS Lett.* (1994) **355** (1), 91
11. Delain, E., et al., *Microsc. Microanal. Microstr.* (1992) **3**, 457
12. Allen, M. J., et al., *Chromosoma* (1993) **102**, 623
13. Fritzsche, W., et al., *Crit. Rev. Eukaryot. Gene Expr.* (1997) **7** (3), 231
14. Fritzsche, W., and Henderson, E., *Scanning Microsc.* (1996) **10** (1), 1
15. Jiao, Y., and Schäffer, T., *Langmuir* (2004) **20** (23), 10038
16. De Grooth, B. G., and Putman, C. A. J., *J. Microsc.* (1992) **168**, 239
17. Rasch, P., et al., *Proc. Natl. Acad. Sci. USA* (1993) **90** (6), 2509
18. Musio, A., et al., *Chromosoma* (1994) **103** (3), 225
19. Tamayo, J., et al., *J. Struct. Biol.* (1999) **128** (2), 200
20. Gobbi, P., et al., *Scanning* (2000) **22** (5), 273
21. Winfield, M., et al., *Chromosome Res.* (1995) **3** (2), 128
22. Fritzsche, W., et al., *Chromosoma* (1994) **103** (4), 231
23. Tamayo, J., *J. Struct. Biol.* (2003) **141** (3), 198
24. Wanner, G., et al., *Chromosoma* (1991) **100**, 103
25. McMaster, T. J., et al., *Genome* (1996) **39** (2), 439
26. Hansma, H. G., et al., *Scanning* (1993) **15** (5), 296
27. Wang, H., et al., *Anal. Sci.* (2000) **16** (12), 1261
28. Putman, C. A., et al., *J. Cytometry* (1993) **14** (4), 356
29. Kalle, W. H. J., et al., *J. Microsc.* (1995) **182** (3), 192
30. Thalhammer, S., et al., (2005), in preparation
31. Fritzsche, W., *Microsc. Res. and Tech.* (1999) **44** (5), 357
32. Stark, R., et al., *Appl. Phys. A* (1998) **66** (Suppl. 1), 579
33. McKay, R. D. G., *Chromosoma* (1973) **44** (1), 1
34. Comings, D. E., *Ann. Rev. Genet.* (1978) **12**, 25
35. Ambros, P. F., and Sumner, A. T., *Cytogenet. Cell Genet.* (1987) **44** (4), 223
36. Harrison, C. J., et al., *Exp. Cell Res.* (1981) **134** (1), 141
37. Thalhammer, S., et al., *J. Microsc.* (2001) **202** (3), 464
38. Yunis, J. J., and Sanchez, O., *Chromosoma* (1973) **44**, 15
39. Heneen, W. K., and Caspersson, T., *Hereditas* (1973) **74** (2), 259
40. Bahr, G. F., and Larsen, P. M., *Adv. Cell. Mol. Biol.* (1974) **3**, 191
41. McMaster, T. J., et al., *Cancer Genet. Cell Genet.* (1994) **76**, 93
42. Ushiki, T., et al., *Arch. Histol. Cytol.* (2002) **65** (5), 377
43. Tamayo, J., *J. Struct. Biol.* (2003) **141** (3), 189
44. Arrighi, F. E., and Hsu, T. E., *Cytogenetics* (1971) **10** (2), 81
45. Sumner, A. T., *Exp. Cell. Res.* (1972) **75** (1), 304
46. Tan, E., et al., *Scanning* (2001) **23** (1), 32
47. Sumner, A. T., and Ross, A., *Scanning Microsc.* (1989) **3** (Suppl.), 87
48. Sanchez-Sweatman, O. H., et al., *Scanning Microsc.* (1993) **7** (1), 97
49. Sumner, A. T., *Scanning Microsc.* (1996) **10** (Suppl.), 165
50. Wanner, G., and Formanek, H., *Chromosome Res.* (1995) **3** (6), 368
51. Hermann, R., and Müller, M., *Arch. Histol. Cytol.* (1992) **55** (Suppl.), 17
52. Nagatani, T., et al., *Scanning Microsc.* (1987) **1** (Suppl.), 901
53. Pawley, J., *Scanning* (1997) **19** (5), 324
54. Rizzoli, R., *Chromosoma* (1994) **103** (6), 393
55. Rizzi, E., *J. Histochem. Cytochem.* (1995) **43** (4), 413
56. Lattanzi, G., *J. Histochem. Cytochem.* (1998) **46** (12), 1435
57. Gobbi, P., *Arch. Histol. Cytol.* (1999) **62** (4), 317
58. Sitti, M., *Proc. IEEE-Nanotechnology Conf.* (2001), 75
59. Scalenghe, F., et al., *Chromosoma* (1981) **82** (2), 205
60. Röhme, D., et al., *Cell* (1984) **36**, 783
61. Fisher, E. M. C., et al., *Proc. Natl. Acad. Sci. USA* (1985) **82** (17), 5846
62. Greenfield, A. J., et al., *Genomics* (1987) **1** (2), 153
63. Senger, G., et al., *Hum. Genet.* (1990) **84** (6), 507
64. Lüdecke, H. J., et al., *Nature* (1989) **338**, 348
65. Johnson, D.C., *Genomics* (1990) **6** (2), 243
66. Jung, C., et al., *Plant Mol. Biol.* (1992) **20**, 503
67. Telenius, H., et al., *Genes-Chromosomes-Cancer* (1992) **4** (3), 257
68. Stein, N., et al., *Plant J.* (1998) **13** (2), 281
69. Pich, U., et al., *Mol. Gen. Genet.* (1994) **243** (2), 173
70. Liu, B., et al., *Plant J.* (1997) **11** (5), 959
71. Chen, Q., and Armstrong, K., *Genome* (1995) **38**, 706
72. Zhou, Y., et al., *Chromosoma* (1999) **108** (4), 250
73. Zhang, L., et al., *Proc. Natl. Acad. Sci. USA* (1992) **89** (13), 5847
74. Nelson, D. L., et al., *Proc. Natl. Acad. Sci. USA* (1989) **86** (17), 6686
75. Thalhammer, S., et al., *J. Struct. Biol.* (1997) **119** (2), 232
76. Weimer, J., et al., *Chromosome Res.* (2001) **9** (5), 395
77. Kao, F. T., and Yu, J. W., *Proc. Natl. Acad. Sci. USA* (1991) **88** (5), 1844
78. Klein, C. A., et al., *Proc. Natl. Acad. Sci. USA* (1999) **96** (8), 4494
79. Monajembashi, S., et al., *Exp. Cell Res.* (1986) **167** (1), 262
80. Ponielies, N., et al., *Chromosoma* (1989) **98**, 351
81. Lengauer, C., et al., *Cytogenet. Cell Genet.* (1991) **56**, 27
82. He, W., et al., *Microsc. Microanal.* (1997) **3**, 47
83. Schermelleh, L., et al., *BioTechniques Int.* (1999) **27**, 362
84. Kubickova, S., et al., *Chromosome Res.* (2002) **10** (7), 571
85. Thalhammer, S., et al., *Chromosome Res.* (2004) **12** (4), 337
86. Hoh, J. H., et al., *Science* (1991) **253**, 1405
87. Vesenka, J., et al., *Ultramicroscopy* (1992) **42-44** (2), 1243
88. Geissler, B., et al., *Scanning* (2000) **22**, 7
89. Falvo, M. R., et al., *Biophys. J.* (1997) **72** (3), 1396
90. Mosher, C., et al., *Scanning Microsc.* (1994) **8** (3), 491
91. Jondle, D. M., et al., *Chromosome Res.* (1995) **3** (4), 239
92. Xu, X.-M., and Ikai, A., *Biochem. Biophys. Res. Commun.* (1998) **248** (3), 744
93. Iwabuchi, S., et al., *Arch. Histol. Cytol.* (2002) **65** (5), 473
94. Thalhammer, S., and Heckl, W. M., *Cancer Genomics Proteomics* (2004) **1** (1), 59
95. Thalhammer, S., *PhD Thesis*, University of Munich (2001)
96. Thalhammer, S., et al., *Acta Microscopica* (2003) **12**, 1
97. Thalhammer, S., et al., *J. Biomed Optics* (1997) **2** (1), 115